Electroweak results from the CMS experiment

L. Lusito[*][†]
Università & INFN Bari, Italy
E-mail: Letizia.Lusito@cern.ch

Results will be presented of electroweak studies with *W* and *Z* bosons with data collected at a center-of-mass energy of 7 TeV by the CMS experiment at the LHC. Measurements include the inclusive *W*, *Z* and Drell-Yan production differential cross sections and measurements of *W* and *Z* production in association with a photon and of diboson production. These results are interpreted in terms of constraints on anomalous triple gauge couplings. Forward-backward asymmetries and charge asymmetries will be presented and also associated jet production and jet multiplicities including *b*-jets in association with *Z* bosons, and of *c*-jets in association with *W* bosons The excellent level of theoretical and experimental understanding of these processes allows electroweak tests at the LHC at an unprecedented level of precision.

LHC on the March,
November 16-18, 2011
Protvino, Moscow region, Russian Federation

---

[*]Speaker.

[†]For the CMS Collaboration

1. Introduction

At the LHC *pp* collider, *W* and *Z* bosons are produced mainly from the scattering of a valence quark and sea anti-quark. The involved Parton Distribution Functions (PDFs) are low ($10^{-3} < x < 10^{-1}$) so that the scattering of a sea quark with a sea anti-quark is also important. *W* and *Z* leptonic decay events have a clear signature and are relatively well-known. As a consequence, they allow to perform precision Standard Model (SM) measurements and to constraint theoretical predictions by limiting the uncertainties in PDFs and by testing NLO and NNLO generators. Electroweak (EWK) bosons are also very powerful tools to understand and calibrate the detector, to measure efficiencies through "tag&probe" methodsand to study the lepton scale and resolution. Moreover, single boson production in association with jets and diboson production are the main backgrounds for most of the Higgs and New Physics searches. It is of fundamental importance to control these backgrounds with very good precision. EWK *W*/*Z* bosons also play a crucial role as benchmark to establish the analysis techniques to search for Higgs and/or New Physics.

For these reasons, a wide EWK physics programme has been developed and carried out at the CMS experiment [1] at the LHC that will be summarized here.

In Section 2 the inclusive cross sections measurements for *W* and *Z* production and leptonic decay in electrons, muons and taus will be presented as well as the *Z* differential cross section and Drell-Yan cross section. In Section 3 the diboson production (*WW*, *WZ*, *ZZ*, *V*+γ) will be discussed.

In Section 4 measurements sensitive to NLO, NNLO effects in the boson production process will be presented like *W*/*Z* production in association with jets, also in association with heavy-flavour jets. Finally, lepton charge asymmetry, weak mixing angle and forward-backward asymmetry will be described in Section 5.

2. *W* and *Z* production

2.1 *W* and *Z* inclusive cross sections

At the LHC, the rate production of single *W* bosons are about 10^6 per fb^{-1}, while the rate for single *Z* boson is approximately 1/10 of that.

W (*Z*) events are characterized by the presence of one (two) isolated lepton with relatively high p_T (> 25 GeV) which is exploited to trigger the event on-line. In case of *W* events, the undetectable neutrino gives origin to an imbalance in the total transverse energy, the missing transverse enery ($\not{E}_T$), which distribution is used to perform a fit from which the W signal is extracted. Another distribution that can be used as well is the transverse mass distribution built from lepton p_T and $\not{E}_T$. Z signal is more easily identificable through the invariant mass peak of the two leptons. Leptons trigger, selection and isolation efficiencies are calculated with tag&probe methods as a function of lepton transverse momentum (p_T) and pseudorapidity (η) while the momentum scale and resolution are calculated from $Z \rightarrow \ell^+ \ell^-$ data. The main background is the QCD multijet production where a quark/gluon jet is misidentified as a lepton or where a real non-isolated lepton is present. QCD can be highly reduced thanks to lepton isolation requirements (sum of tracks and calorimeter deposits around lepton direction, calculated in a cone of aperure $\Delta r = \sqrt{(\Delta\phi)^2 + (\Delta\eta)^2} < 0.3$, normalized to lepton p_T) while its remaining contribution to signal can be measured in data in control
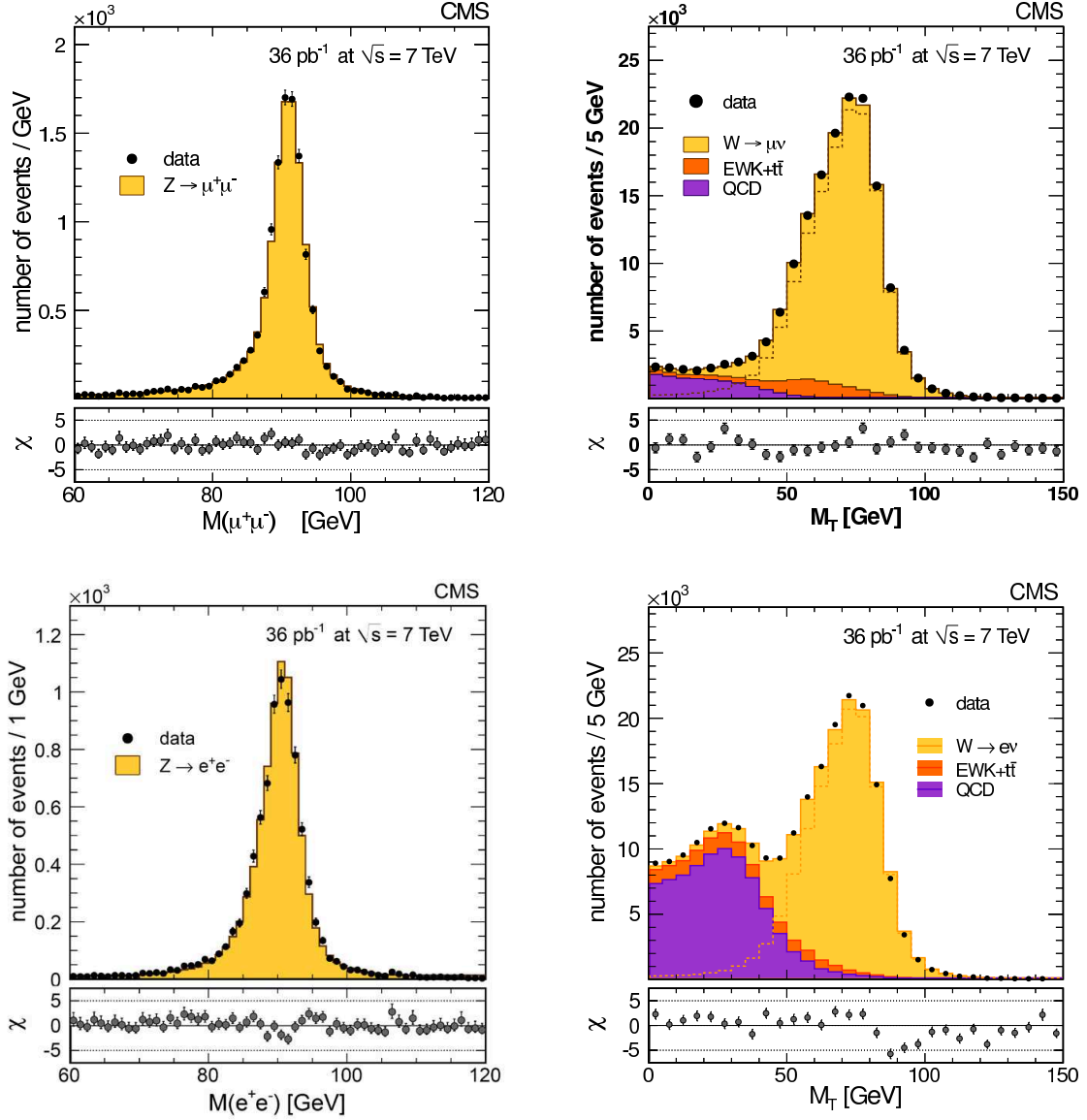
Figure 1: Control plots for the *W/Z* cross section measurement: invariant mass distribution of the two muons in $Z \rightarrow \mu^+\mu^-$ events (top left), transverse mass distribution of muon and E_T in $W \rightarrow \mu\nu$ events (top right), invariant mass distribution of the two electrons in $Z \rightarrow e^+e^-$ events (bottom left), transverse mass distribution of electron and missing transverse energy in $W \rightarrow e\nu$ events (bottom right).

regions (e.g., an anti-isolated sample), since its simulation with simple LO and Parton Shower (PS) Monte Carlo (MC) is not reliable and the lepton fake rate is very much dependent on the details of the detector. The EWK background can be measured mostly from MC simulation and is composed of $t\bar{t} \rightarrow Wb\bar{b}$, dibosons, *W/Z* to leptonically decaying taus events or events where one lepton is outside the geometrical detector acceptance. An inclusive *W* and *Z* signal extraction has been performed on the first data by CMS [2]. Control plots for the *W/Z* cross section measurement have been reported in Figure 1.

The measured cross sections are in good agreement with theoretical prediction at NNLO based
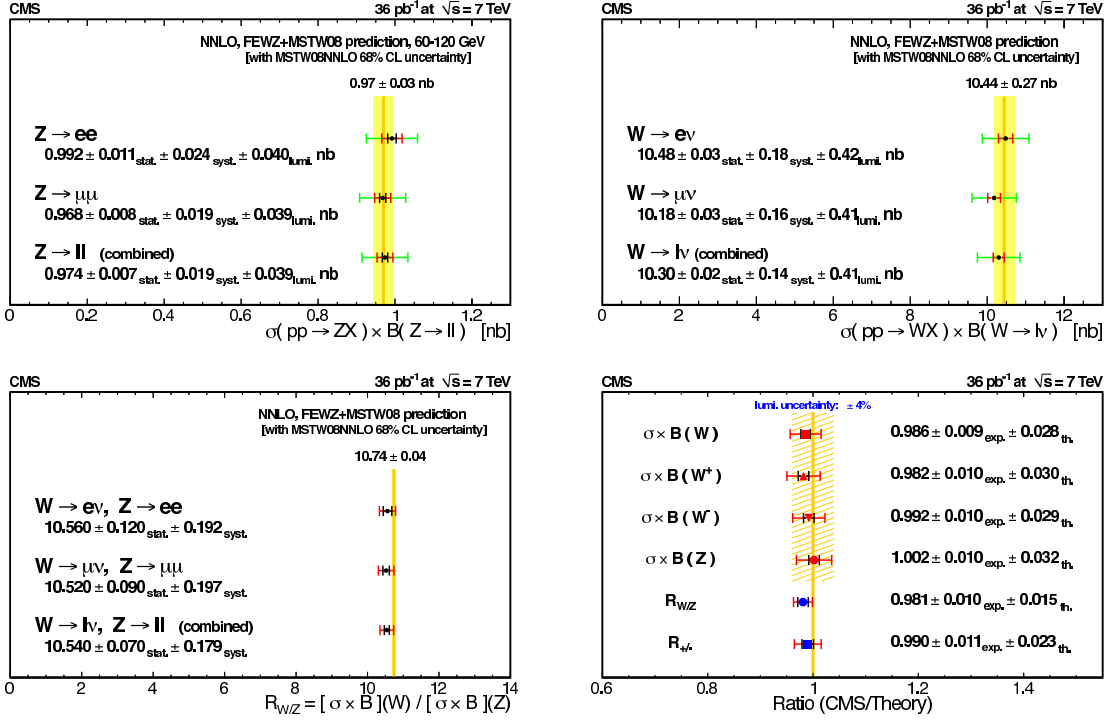
Figure 2: Experimental *W*/*Z* inclusive cross sections and comparison with theoretical predictions at NNLO.

on recent parton distribution functions as shown in Figure 2.

With 35 pb^{-1} the statistical error is already negligible and, with the exception of the luminosity uncertainty (4%), the other experimental systematics (dominated by the $\not{E}_T$ resolution and the lepton efficiencies) are lower (1%) than the theoretical uncertainty ($\leq$3%).

2.2 *W* and *Z* decaying to taus

In the context of SM, $Z \rightarrow \tau^+\tau^-$ is an important source of high energetic tau leptons allowing a precise measurement of τ identification efficiencies and commissioning of τ triggers. It is also an irreducible background in many searches beyond SM. In CMS, tau leptons are reconstructed by using the HPS algorithm based of Particle Flow candidates (obtained by combining tracker and calorimeter measurements). Figure 3 reports the comparison between the cross section values obtained for the $Z \rightarrow \tau^+\tau^-$ channel, the theoretical predictions and the inclusive cross sections values for the muon and electron channels [3]. The tau ID efficiency value has been extracted from a fit obtained by contraining the $\sigma(pp \rightarrow Z) \times BR(Z \rightarrow \tau^+\tau^-)$. The main systematics in this channel is the tau identification efficiency determined with this fit on data and amounts to 23%.

2.3 *Z* differential cross section

The very large *Z* production at the LHC hence the large available statistics of *Z* events allows to study differential cross sections as a function of lepton rapidity (y) and p_T, important to test different theoretical predictions. The comparison is performed for muon and electron channels after an unfolding procedure aimed at correcting for resolution and final-state radiation [4]. Figure 4

4
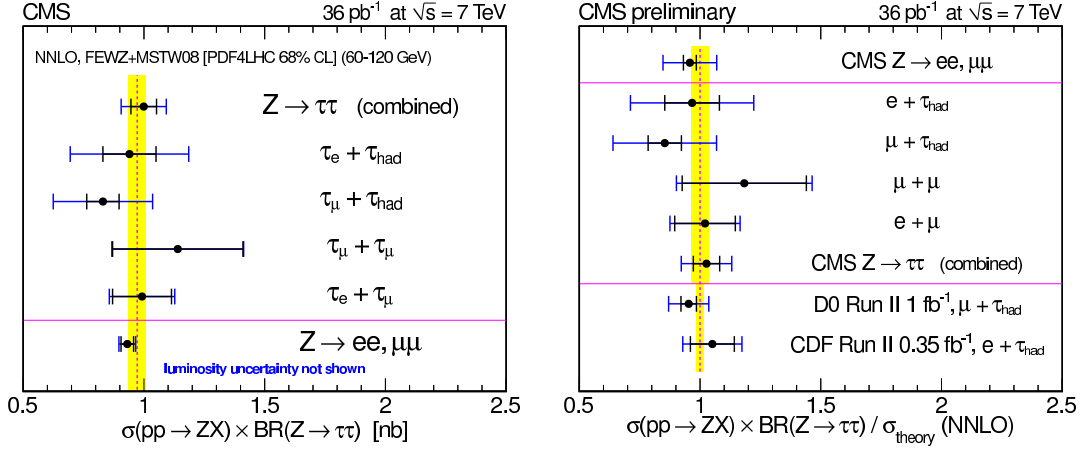
Figure 3: Comparison between the cross section values obtained for the $Z \to \tau^+\tau^-$ channel, the theoretical predictions and the inclusive cross sections values for the muon and electron channels measured by CMS.
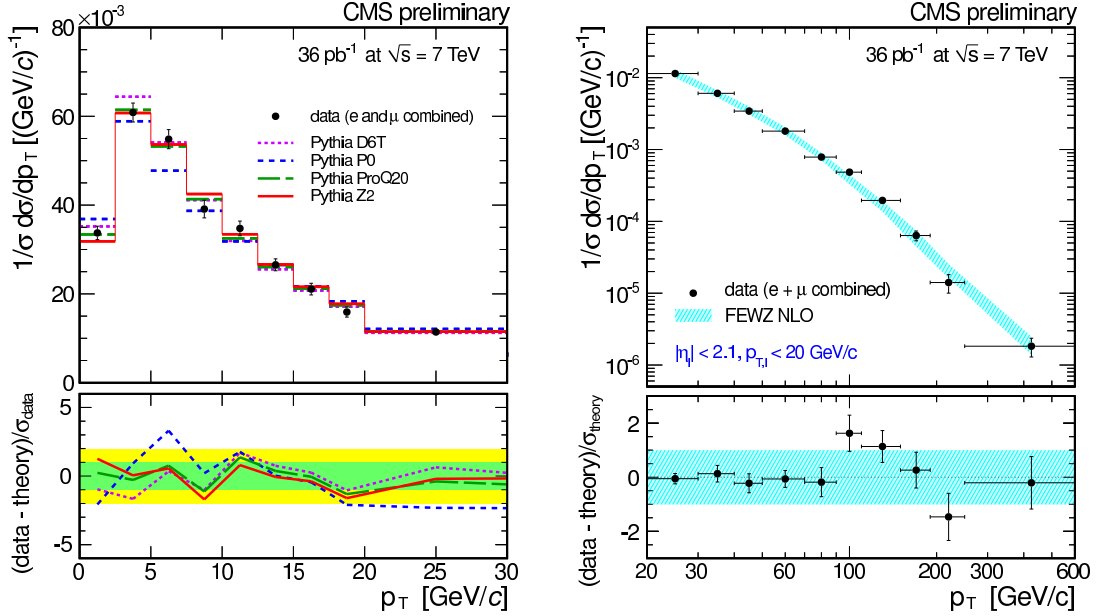
Figure 4: The combined electron and muon measurement of the Z boson transverse momentum distribution (points) and the predictions of four PYTHIA tunes and of POWHEG interfaced with PYTHIA using the Z2 tune (histograms) in the low-p_T, region sensitive to Pythia (top), and in the high-p_T region sensitive to FEWZ (bottom). The lower portion of the figure shows the difference between the data and the simulation predictions divided by the uncertainty σ on the data.

shows the differential Z cross section as a functions of lepton p_T for different Pythia tunes and FEWZ predictions; the low-p_T region is where the non-perturbative conditions multiple (soft gluon radiations dominate), which are typically described by Pythia, while the high-p_T region is where the perturbative contributions dominate (hard gluon emission), described by FEWZ.

2.4 Drell-Yan cross section

The Drell-Yan differential cross section distribution, outside the Z resonance region, is important because it is sensitive to PDFs assumptions, EWK corrections and can be eventually modified by new physics effects. The dilepton differential cross section distribution as a function of invariant mass normalized to the cross-section in the Z region (60<M(ℓ,ℓ)<120 GeV), unfolded for resolution, corrected for acceptance, efficiency and final state radiation (FSR) effects (not included in FEWZ) is shown in Figure 5 [5]. A full NNLO approach is adopted since a substantial fraction of the selected events in the very low invariant mass bins correspond to high-p_T lepton pairs accompanied by hard jets. Experimental results are in good agreement with the predictions from FEWZ.
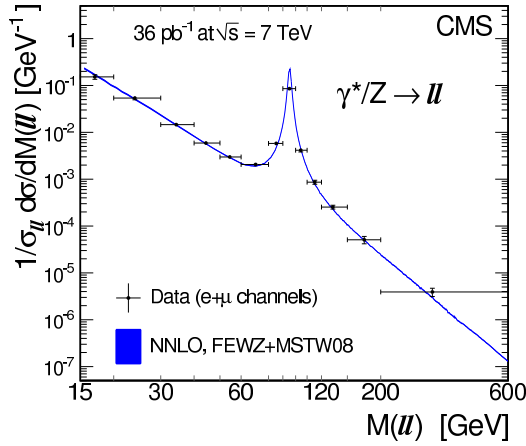

Figure 5: CMS normalized dilepton differential cross section distribution as a function of the dilepton mass.

3. Diboson production

3.1 WW, WZ and ZZ cross sections

Triggered by Higgs boson searches, the production of pairs of heavy gauge bosons has been analyzed at CMS measuring the WW, WZ and ZZ cross sections [6]. All the analyses focus on leptonic decay channels, which provide pure signatures, but also have low branching fractions compared to semi-leptonic channels. In this way, rather clean signals are obtained applying selection criteria to reject the major background contributions: W plus jets, top backgrounds, Drell-Yan, $Z \to \tau^+\tau^-$, multijet events. The electron and muon identification criteria are similar to the ones used in inclusive analyses while the dominant backgrounds are controlled via data-driven methods.

In the WW channel 626 events have been selected in data against a signal+background MC predictions of 568.6 ± 52.2. The WZ channel is cleaner than WW. For $\mathscr{L} = 1\,\text{fb}^{-1}$, the typical yields are of $\approx 70 - 80$ events with ≈ 10- 15% background in the fully leptonic case. ZZ is the
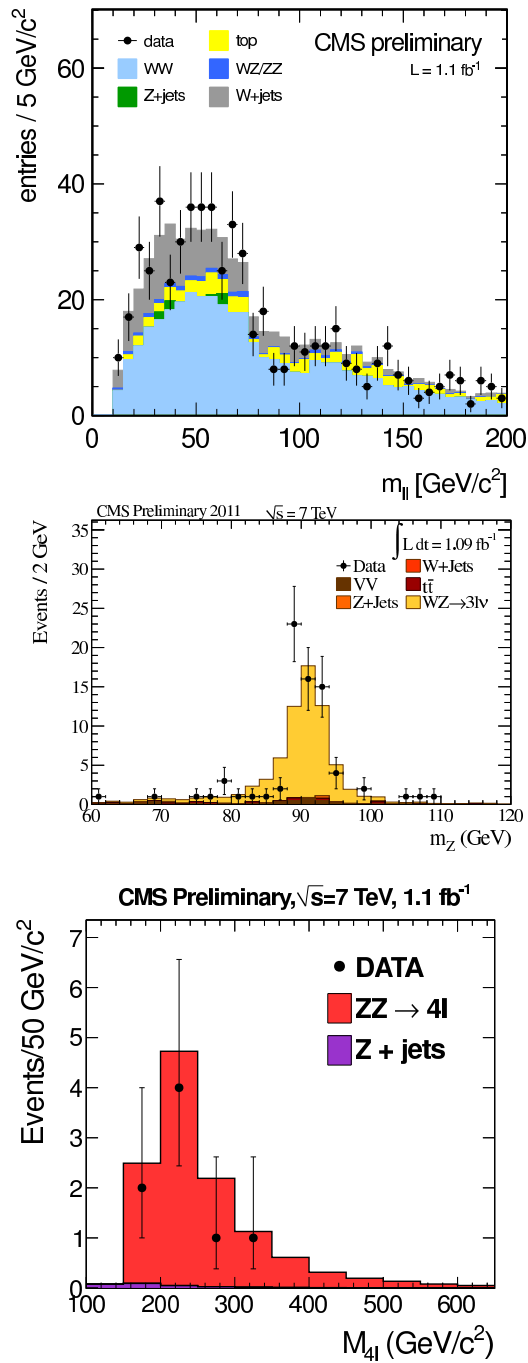
Figure 6: Invariant mass of the two leptons in selected WW events (top), invariant mass of Z boson in selected WZ events (middle) and four-lepton invariant mass distribution for ZZ selected events (bottom).

cleanest channel, thanks to the availability of a double Z mass constraint. For $\mathcal{L} = 1\ fb^{-1}$ the typical yields are of ≈ 10 events with almost negligible backgrounds

Figure 6 shows the invariant mass of the two leptons in selected WW events (top plot), the invariant mass of Z boson in selected WZ events (middle plot) and four-lepton invariant mass

distribution for ZZ selected events (bottom plot).

The experimental values of diboson production cross section as measured by CMS are:

- $\sigma(pp \to WW + X) = 55.3 \pm 3.3$ (stat.) ± 6.9 (syst.) ± 3.3 (lumi.) pb,
  SM expectation: 43.0 ± 2.0 pb at NLO

- $\sigma(pp \to WZ + X) = 17.0 \pm 2.4$ (stat.) ± 1.1 (syst.) ± 1.0 (lumi.) pb,
  SM expectation: 19.790 ± 0.088 pb at NLO

- $\sigma(pp \to ZZ + X) = 3.8^{+1.5}_{-1.2}$ (stat.) ± 0.2 (syst.) ± 0.2 (lumi.) pb,
  SM expectation: 6.4 ± 0.6 pb at NLO

3.2 W/Z and photons

The production of W and Z bosons in conjunction with photons (V+γ events) is important because the contribution of the SM triple gauge couplings to these channel is small ($W+\gamma$) or zero ($Z+\gamma$) as these final states are predominantly produced by initial and final state radiation of photons while anomalous triple gauge couplings (aTGC) are expected to show most prominently at high transverse momenta of the photon. Z bosons are selected by requiring two isolated leptons with $p_T > 20$ GeV. Only reconstructed Z bosons with an invariant mass greater than 50 GeV are used. W bosons are reconstructed with an isolated lepton with $p_T > 20$ GeV and $\not{E}_T > 25$ GeV. For both analyses, photons must have $p_T > 10$ GeV and must respect the condition $\Delta R(\gamma, \ell) = \sqrt{(\Delta\eta)^2 + \Delta\phi)^2)} > 0.7$. These requirements define also the phase space used for cross section measurements, giving the following results [7]:

- $\sigma(pp \to W\gamma + X) \times \mathrm{BR}(W \to \ell\nu) = 56.3 \pm 5.0$ (stat.) ± 5.0 (syst.) ± 2.3 (lumi.) pb, SM expectation: 49.4 ± 3.8 pb at NLO

- $\sigma(pp \to Z\gamma + X) \times \mathrm{BR}(Z \to \ell\ell) = 9.4 \pm 1.0$ (stat.) ± 0.6 (syst.) ± 0.4 (lumi.) pb, SM expectation: 9.6 ± 0.4 pb at NLO

Figure 7 shows the photon transverse momentum distribution in $W + \gamma$ events as observed in data and theoretical predictions for an anomalous coupling. Since no excess in these channel has been observed by CMS, limits on aTGC have been set.

4. W and Z production in association with jets

4.1 V+jets

The production of W and Z bosons in association with hadronic jets allows to test perturbative NLO QCD calculations, to provide an estimate of background for searches of SM Higgs boson, BSM or top quarks, to probe different PDFs through flavour specific final states. The selection criteria are similar to inclusive W/Z cross section analyses while jets are reconstructed with the anti-kT algorithm with $\Delta R = 0.5$. Only jets with $E_T > 30$ GeV have been considered. Data are unfolded for detector effect. To minimize the systematic uncertainties (dominated by Jet Energy Scale, PileUp effects) the following ratios have been measured [7]:
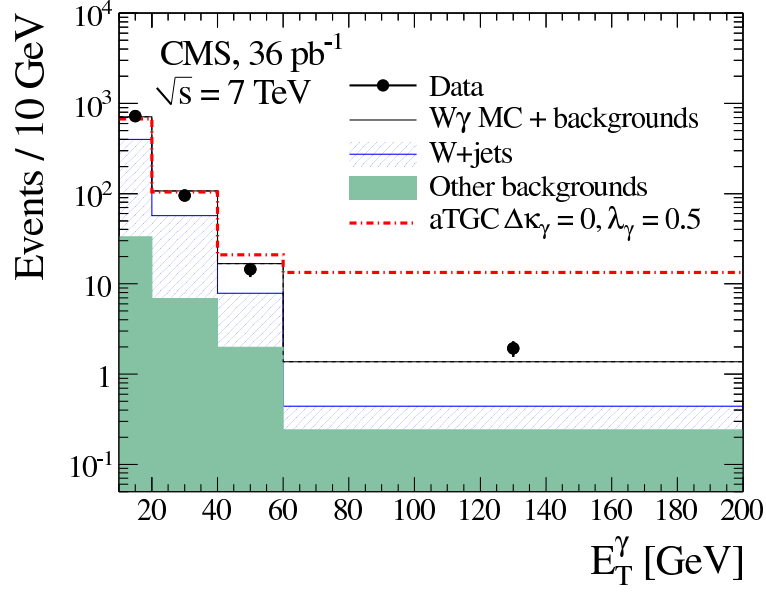
Figure 7: Photon transverse momentum distribution in $W + \gamma$ events as observed in data (black points) and theoretical predictions for an anomalous coupling (dash-dotted line).
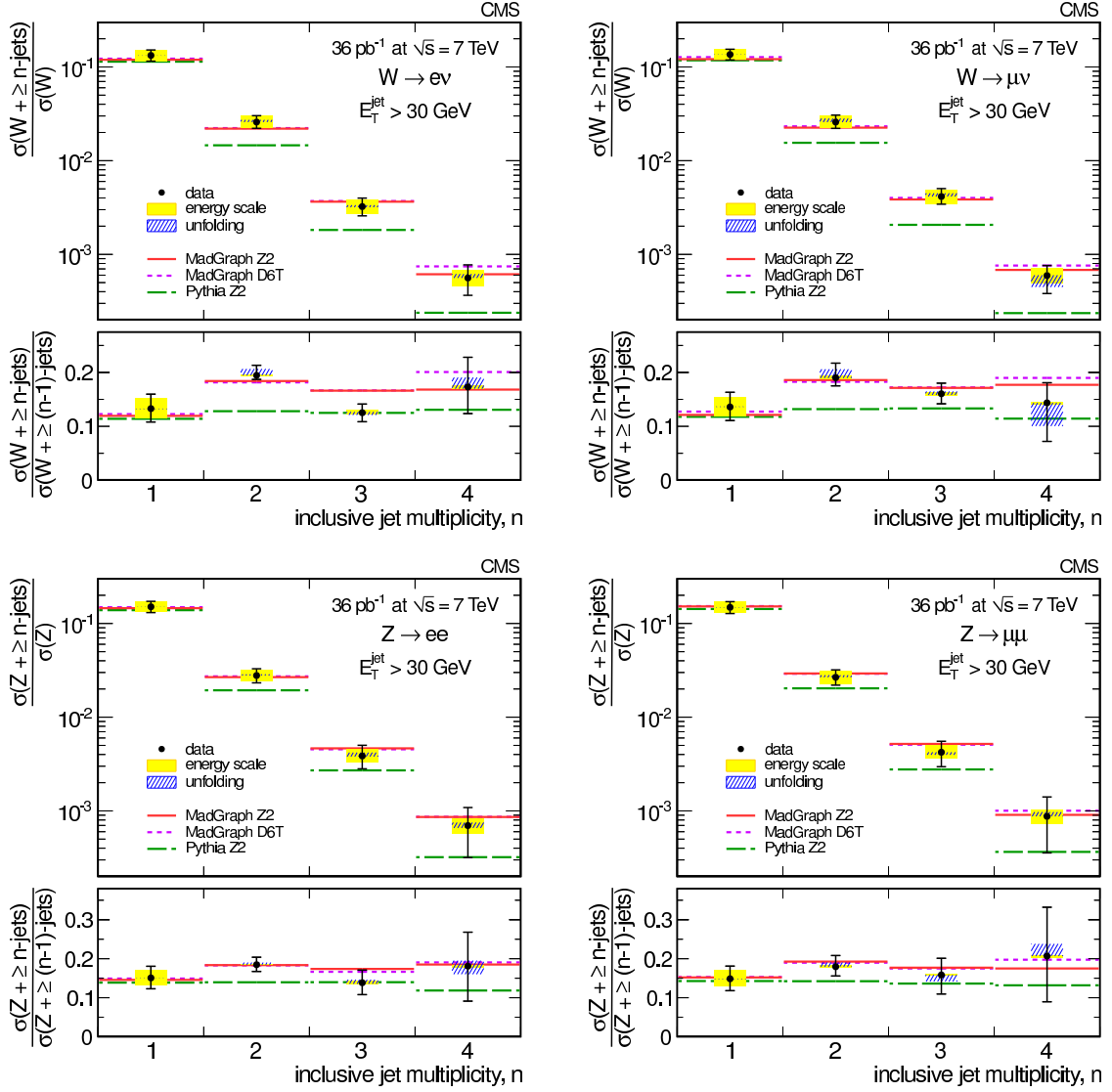
- $\sigma(V + n\,jets) / \sigma(V)$

- $\sigma(V + n\,jets) / \sigma(V + (n-1)\,jets)$

- $\sigma(W + jets) / \sigma(Z + jets)$

A good agreement with MadGraph for W and Z is observed even if at high jet multiplicities Z has large statistical uncertainty compared to W. Figure 8 reports the cross sections $\sigma(V + \geq n\text{-jets})$ distributions normalized to the inclusive V cross section $\sigma(V + \geq 0\text{-jets})$ as a function of the inclusive number of jets n up to n = 4, and the ratio $\sigma(V + \geq n\text{-jets})/\sigma(V + \geq (n-1)\text{-jets})$, for V = W (top plots) and Z (bottom plots) in the electron (left) and muon (right) channels. Data are compared to theory predictions obtained with MadGraph interfaced with Pythia (ME+PS) with two different tunes, D6T and Z2, as well as with Pythia with the Z2 tune.

The Berends-Giele scaling according to which the ratio $C(n) = \sigma(V + \geq n\text{-jets})/\sigma(V + \geq (n+1)\text{-jets})$ is approximately constant for $n \geq 1$ has been tested by fitting experimental data with the constraint $C(n) = \alpha + \beta \times n$ and representing them in the (α, β) plane, separately for the electron and muon channels. The results of the fit is that β is close to zero as expected, confirming that the ratio $C(n)$ is indipendent on the number of jets n.

4.2 $Z + b$-**jets**

Z production has been studied also when it is associated to at least one jet identified as produced by a b quark. This allows to investigate the two main production mechanisms: a b pair produced from quark-quark or gluon-gluon scattering (fixed flavour) or a single b quark produced

Figure 8: Cross sections $\sigma(V + \geq$ n-jets) normalized to the inclusive V cross section $\sigma(V + \geq$ 0-jets) as a function of the inclusive number of jets n up to n = 4, and the ratio $\sigma(V + \geq$ n-jets)/$\sigma(V + \geq$ (n-1)-jets), for V = *W* (top plots) and *Z* (bottom plots) in the electron (left) and muon (right) channels. Data are compared to theory predictions obtained with MadGraph interfaced with Pythia (ME+PS) with two different tunes, D6T and Z2, as well as with Pythia with the Z2 tune.

at partonic level (variable flavour). The purity of the *b*-tagging selection has been determined from data using a fit to the distribution of the invariant mass of tracks associated to the secondary vertex.

The ratio of Z production cross section in association with a *b*-jet and in association with a generic jet has been found in agreement with NLO predictions [8]:

- $\sigma(Z + b)/\sigma(Z+$jet)$= 0.054 \pm 0.016$ for $Z \rightarrow e^+ e^-$,
  SM expectation: 0.043 ± 0.005 pb at NLO

- $\sigma(Z + b)/\sigma(Z+$jet)$= 0.046 \pm 0.014$ for $Z \rightarrow \mu^+ \mu^-$,

SM expectation: 0.047 ± 0.005 pb at NLO

4.3 $W + c$-jets

The production of W boson in association to a jet produced by a c quark provides important information on the strange and anti-strange quark parton density functions of the proton at the EWK scale. Using muonic decays of the W boson and lifetime tagging techniques to extract the charm fraction in the selected W + jet sample, the following ratios are obtained [9]:

- $\sigma(W^{+} + \bar{c} + X)/\, \sigma(W^{-} + c + X) = 0.92 \pm 0.19$ (stat.) ± 0.04 (syst.),
  SM expectations: 0.91 ± 0.04 at NLO

- $\sigma(W + c + X)/\, \sigma(W + \text{jet} + X) = 0.143 \pm 0.015$ (stat.) ± 0.024 (syst.),
  SM expectations: 0.13 ± 0.02 at NLO

5. Asymmetries

5.1 W charge asymmetry

Of particular interest is the charge asymmetry along the beam direction that is observed in W boson production. It allows to probe the difference between quark and anti-quark density. At CMS the W^{+}/W^{-} ratio as a function of the lepton η has been measured since many systematics cancel in the ratio [10]:

$$\mathscr{A}(\eta) = \frac{\frac{d\sigma}{d\eta_{\ell}}(W^{+} \to \ell^{+}\nu) - \frac{d\sigma}{d\eta_{\ell}}(W^{-} \to \ell^{-}\nu)}{\frac{d\sigma}{d\eta_{\ell}}(W^{+} \to \ell^{+}\nu) + \frac{d\sigma}{d\eta_{\ell}}(W^{-} \to \ell^{-}\nu)}$$

The results are reported in Figure 9.

5.2 Weak mixing angle

The vector coupling of fermions is directly related to the weak mixing angle or Weinberg angle: $g_{V}^{f} = I_{3}^{f}$; $g_{A}^{f} = I_{3}^{f} - 2q_{f} \cdot sin^{2}\theta_{W}$ The effective weak mixing angle is extracted from di-muon data using an unbinned maximum-likelihood fit based on the di-lepton mass, rapidity and decay angle observables. In this way, from the dominant $u\bar{u}$, $d\bar{d} \to \gamma^{*}/Z \to \mu^{+}\mu^{-}$ process, the effective weak mixing angle parameter is measured to be $sin^{2}\theta_{eff} = 0.2287 \pm 0.0020$ (stat.) ± 0.0025 (syst.) [11]. This result is consistent with measurements from other processes, as expected within the standard model and with higher precision measurements at previous collider experiments (LEP, Tevatron, Hera) and in neutrino/antineutrino deep inelastic scattering on nucleons experiments (NuTeV).
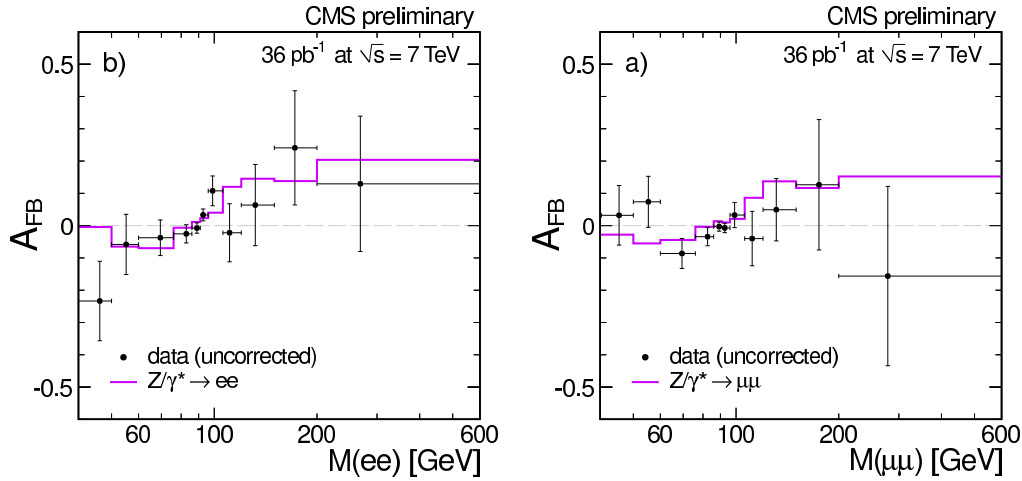
5.3 Forward-Backward Asymmetry

The forward-backward asymmetry AFB, defined as:
$A_{FB} = (\sigma_{F} - \sigma_{B})/(\sigma_{F} + \sigma_{B}) = (N_{F} - N_{B})/(N_{F} + N_{B})$
for opposite sign lepton pairs ($e^{+}e^{-} and \mu^{+}\mu^{-}$) produced via an intermediate Z/γ^{*} has been measured as a function of mass in $40 < M(\ell,\ell) < 600$ GeV range. The results have been reported in
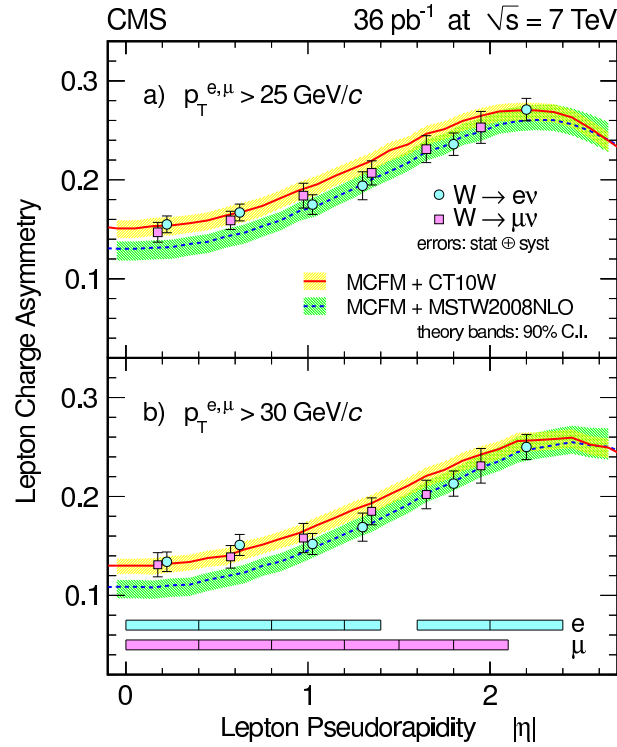
Figure 9: Lepton charge asymmetry in six bins of absolute lepton pseudorapidity $|\eta|$, in the $W \to e\nu$ channel (light blue points) and the $W \to \mu\nu$ channel (light pink points). Different thresholds on the lepton transverse momentum have been applied: 25 GeV (top); 30 GeV (bottom).

Figure 10: Forward-backward asymmetry AFB, for opposite sign lepton pairs: e^+e^- (top) and $\mu^+\mu^-$ (bottom) as a function of mass in $40 < M(\ell,\ell) < 600$ GeV range.

Figure 10. This measure is important because around Z pole, A_{FB} is dominated by interference of vector and axial vector coupling of Z to quarks while, away from Z-pole, A_{FB} is dominated by $Z/\gamma*$
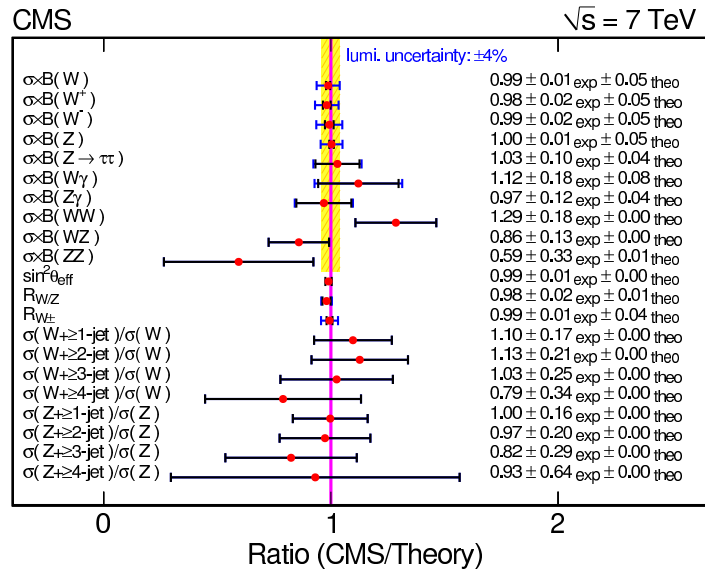
Figure 11: Ratio of CMS electroweak measurements to SM theoretical predictions.

interference and it is sensitive to new physics [12].

6. Summary of CMS EWK results and conclusions

CMS produced many EWK measurements with the first 36 pb^{-1} (results with 1.1 fb^{-1} start to become available) of LHC data at 7 TeV. Precision measurements of inclusive *W* and *Z* production cross-section with large statistics constitute an important test of the Standard Model at the energy scale of LHC. Detailed studies of differential cross-sections and many observables like asymmetries, V+jets (also with heavy-flavour jets) dibosons productions have been reported. All measurements are in agreement with theoretical predictions from the SM. A summary of the ratios of CMS measurements to the SM predictions is shown in Figure 11. Even if many measurements are already limited by systematic uncertainties, the increasing integrated luminosity will allow to have access to more rare SM processes.

References

[1] CMS Collab., JINST **3**, S08004 (2008).

[2] CMS Collab., J. High Energy Phys. **10**, 132 (2011).

[3] CMS Collab., J. High Energy Phys. **08**, 117 (2011).

[4] CMS Collab., *Measurement of the Rapidity and Transverse Momentum Distributions of Z Bosons in pp Collisions at $\sqrt{s} = 7$ TeV*, hep-ex:1110.4973; CMS-EWK-10-010, CERN, Geneva, 2010; CERN-PH-EP-2011-169, CERN, Geneva, 2011.

[5] CMS Collab., Phys. Lett. B **701**, 535 (2011).

[6] CMS Collab., *Measurement of the WW, WZ and ZZ cross sections at CMS*, CMS-PAS-EWK-11-010, CERN, Geneva, 2011.

[7] CMS Collab., *Jet Production Rates in Association with W and Z Bosons in pp Collisions at* $\sqrt{s} = 7$ *TeV*, hep-ex:1110.3226; CMS-EWK-10-012, CERN, Geneva, 2010; CERN-PH-EP-2011-125, CERN, Geneva, 2011; J. High Energy Phys. **01**, 010 (2012).

[8] CMS Collab., *Observation of Z+b*, CMS-PAS-EWK-10-015, CERN, Geneva, 2011.

[9] CMS Collab., *Study of associated charm production in W final states at* $\sqrt{s} = 7$ *TeV*, CMS-PAS-EWK-11-013, CERN, Geneva, 2011.

[10] CMS Collab., J. High Energy Phys. **04**, 050 (2011).

[11] CMS Collab., Phys. Rev. D **84**, 112002 (2011)

[12] CMS Collab., *Forward-backward asymmetry of Drell-Yan pairs*, CMS-PAS-EWK-11-011, CERN, Geneva, 2011.

PoS(IHEP-LHC-2011)009